ARTICLE

Enhanced Electrochemical Performances of $LiFePO_4$/C via V and F Co-doping for Lithium-Ion Batteries

Tao-tao Zhan, Chao Li, Yun-xia Jin, Shun-hua Xiao*

College of Chemistry and Bioengineering, Guangxi Key Laboratory of Electrochemical and Magnetochemical Functional Materials, Guilin University of Technology, Guilin 541006, China

(Dated: Received on July 24, 2015; Accepted on November 10, 2015)

Based on the method of *in situ* polymerization synthesis combined with two-step sintering process, $LiFe_{1-x}V_x(PO_4)_{(3-y)/3}F_y$/C was prepared. The effects of V and F co-doping on the structure, morphology, and electrochemical performances of $LiFePO_4$/C were investigated by X-ray diffraction, Fourier transform infrared spectra, scanning electron microscope, charge/discharge tests, and electrochemical impedance spectroscopy, respectively. The results indicated that the V and F co-doping did not destroy the olivine structure of $LiFePO_4$/C, but it can stabilize the crystal structure, decrease charge transfer resistance, enhance Li ion diffusion velocity, further improve its cycling and high-rate capabilities of $LiFePO_4$/C.

Key words: $LiFePO_4$/C, $LiFe_{1-x}V_x(PO_4)_{(3-y)/3}F_y$/C, Electrochemical performances, Diffusion velocity

I. INTRODUCTION

Nowadays, Li-ion battery has attracted much attentions for its great potential to be used as power sources for electric vehicles and hybrid electric vehicles [1, 2]. Among various lithium-ion batteries, the ordered olivine lithium iron phosphate $LiFePO_4$ has been recognized as one of the most promising cathode materials for its nontoxicity, low cost, environmental friendliness, long cycling life and high theoretical capacity [3−5]. A lot of researches [6−8] about the synthesis process, structure, electrochemical performance, and applications has been completed, then great progress in physical, chemical properties and synthesis technology had been achieved [9, 10]. However, the poor rate capacity of $LiFePO_4$ resulting from both the poor electronic conductivity (1×10^{-10} S/m) [11, 12] and low Li^+ diffusion coefficient (1×10^{-14} cm^2/s) [13] limits its practical application. So far, various effective methods have been introduced to solve these above problems by using coating particles [14−18], reducing particles sizes [19, 20], and doping with guest element [21−23], *etc.*

Besides carbon coating [24−28] which can effectively improve the electronic conductivity of $LiFePO_4$, cation doping is another effective method to increase the ion electronic conductivity of $LiFePO_4$, such as the doping at Fe-site for $LiFe_{1-x}M_xPO_4$ (M=V, Ni, Co, Ti, Al, *etc.*) [29−32]. Similarly, the anion doping can also enhance the electrochemical performances of $LiFePO_4$, such as the rate capability and cycling life [33−41]. Although the study of anion doping was not as full as cation doping, it should not be neglected.

In order to enhance the electrochemical performance of $LiFePO_4$, in this work, the $LiFePO_4$/C sample with V cation and F anion co-doping at different sites was synthesized via the method of *in situ* polymerization synthesis combined with two-step sintering process. The effects of co-doping with different amount on the structure, morphology, and electrochemical property of $LiFePO_4$/C have been studied in detail.

II. EXPERIMENTS

$FePO_4$/PANI (polyaniline) precursor was prepared by *in situ* polymerization technology. 100 mL of $Fe(NO_3)_3$ solution (0.25 mol/L) was added into 200 mL of $(NH_4)_2HPO_4$ (0.125 mol/L) solution with 1 mL aniline, then the pH of the solution was adjusted to 2.1 and stirred for 12 h. The $FePO_4$/PANI precipitate was achieved by filtering and drying under 60 °C vacuum environment for 24 h.

Pristine $LiFePO_4$/C and $LiFe_{1-x}V_x(PO_4)_{(3-y)/3}F_y$ (x=0.04, y=0.02) powders were synthesized as follows: the stoichiometric amounts of $CH_3COOLi{\cdot}2H_2O$, LiF, NH_4VO_3, 10wt% ascorbic acid and the prepared $FePO_4$/PANI were mixed and milled. After annealing at 350 °C for 5 h under argon atmosphere, 10wt% glucose was added and milled again, and then the mixture was annealed at 650 °C for 10 h under argon atmosphere.

*Author to whom correspondence should be addressed. E-mail: xiaoshunhua@glite.edu.cn, Tel.: +86-13457672829, FAX: +86-773-5898551.

TABLE I Lattice parameters of the samples.

Sample	a/Å	b/Å	c/Å	V/Å^3
$LiFePO_4/C$	10.3019	5.9951	4.6882	289.57
$LiFe_{0.96}V_{0.04}(PO_4)_{2.98/3}F_{0.02}/C$	10.3002	6.0037	4.6910	290.08

The phase identification of powders was conducted with X-ray diffraction measurement (XRD, Panalytical X'Pert PRO MRD, Holland) with a Cu Kα radiation operated at 40 kV and 40 mA. The diffraction data for Rietveld refinement were obtained at 2θ=10°−70°, with a step size of 0.013°. The morphology was evaluated by field emission scanning electron microscopy (FE-SEM S-4800, Hitachi High-Technologies). The FTIR spectra of $LiFePO_4/C$ were recorded with a FTIR spectrometer (Nicolet iS10, Thermo Fisher Scientific).

The electrochemical experiments were performed using button cells. The cathode consisted of a mixed material of active materials, carbon black and poly(vinyl difluoride) (PVDF) with mass ratio of 8:1:1 in *N*-methyl-2-pyrrolidone solvent. Metallic lithium foil was used as the anode electrode. Celgard 2300 polyethylene film was used as separator. 1 mol/L $LiPF_6$ solution in ethylene carbonate and dimethyl carbonate (volume ratio of 1:1) was used as electrolyte. The electrochemical performance measurements were carried out with CR2025 coin cells in an argon-filled glove box. Charge/discharge tests were performed using the LAND batteries test system (CT2001A, Wuhan Land Electronic Co., Ltd., China) with different current densities. Cyclic voltammetry (CV) were performed on an electrochemical working station (CHI660D, Shanghai Chenhua Co., Ltd., China) between 2.5 and 4.2 V.

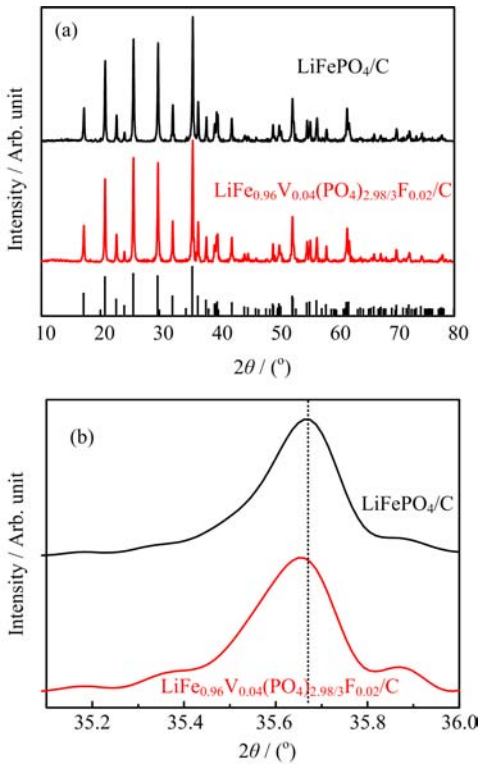

FIG. 1 (a) XRD patterns of pristine and doped $LiFePO_4/C$ samples and (b) magnification of XRD patterns in the field of 35°−36°.

III. RESULTS AND DISCUSSION

Figure 1 shows XRD patterns of the pristine and V and F co-doped $LiFePO_4/C$. All dominant diffraction lines of samples can be indexed as an olivine phase space group Pnma (JCPDS card No.83-2092), which were consistent with the previous reports [42, 43]. Typical diffraction peaks of carbon, vanadium and fluorine can not be found, indicating that the contribution of the carbon was less or the carbon existed in amorphous form, and the elements V and F probably entered into the lattice of $LiFePO_4$ rather than form impurities. Both samples had narrow diffraction peaks, which indicated good crystallinity degree. Figure 1(b) shows the magnification of the field of 35°−36°, there was a very slight shift to lower angle for the doped sample, it was in line with convention that the diffraction peak with larger unit cell volume would shift towards lower diffraction angles in XRD pattern.

What's more, the crystal lattice parameters were calculated by MDI Jade 5.0, and the results are listed in Table I. As shown, that V and F doping led to slight increase of lattice parameters. The doped sample expanded the b and c by 0.14% and 0.06% respectively, and shrinked a by 0.017%, which indicated that the V and F entered into the crystal structure and caused lattice distortion in the $LiFePO_4/C$ unit cell. The volume of the unit cell of the doped sample was slightly larger than that of the pristine $LiFePO_4/C$, which was beneficial to intercalation and deintercalation for Li ion.

The details of the chemical bonding in the $LiFe_{1-x}V_x(PO_4)_{(3-y)/3}F_y/C$ samples were investigated in the FTIR spectra, as shown in Fig.2. The FTIR spectra exhibited many prominent and narrow multiple vibration bands in the range of 500−2000 cm^{-1}. For two samples, the absorption bands centered at 635.59, 966.09, 1051.99, 1095.55, and 1138.06 cm^{-1} corresponded to the symmetric and asymmetric modes of $(PO_4)^{3-}$ groups. In the lower wave number region, the absorptions at 471.57, 501.10, 548.76, 576.39 cm^{-1} were attributed to the symmetric and asymmetric bending modes of P−O bonds [44]. In addition, the absorption at 1630 cm^{-1} can be as-

DOI:10.1063/1674-0068/29/cjcp1507163

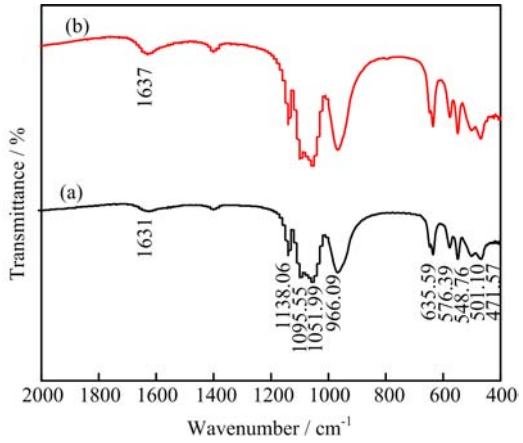

FIG. 2 FTIR spectrum of $LiFe_{1-x}V_x(PO_4)_{(3-y)/3}F_y/C$. (a) $LiFePO_4/C$, (b) $LiFe_{0.96}V_{0.04}(PO_4)_{2.98/3}F_{0.02}/C$.

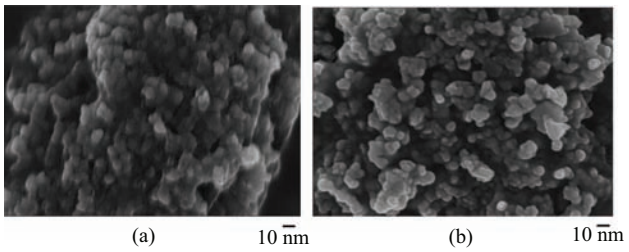

FIG. 3 SEM images of $LiFe_{1-x}V_x(PO_4)_{(3-y)/3}F_y/C$ samples. (a) x=0, y=0, (b) x=0.04, y=0.02.

signed to the stretching vibration of the aromatic ring C=C bonds in grapheme. Most importantly, that the peaks of $LiFe_{0.96}V_{0.04}(PO_4)_{2.98/3}F_{0.02}/C$ samples shifted slightly to higher band numbers, implying the doping ions entrance and the resulted absorption shift.

SEM images of $LiFe_{1-x}V_x(PO_4)_{(3-y)/3}F_y/C$ samples are shown in Fig.3. It indicated that the morphology of $LiFePO_4/C$ particles was sphere-like similar to that of $LiFe_{0.96}V_{0.04}(PO_4)_{2.98/3}F_{0.02}/C$. It showed that the *in situ* polymerization synthesis method can effectively control the size and morphology of samples, and the V and F doping did not result in evident influence on the particles morphology. In comparison, $LiFe_{0.96}V_{0.04}(PO_4)_{2.98/3}F_{0.02}/C$ sample presented better dispersion and uniformity than that of $LiFePO_4/C$ sample.

Rate capabilities of $LiFe_{0.96}V_{0.04}(PO_4)_{2.98/3}F_{0.02}/C$, $LiFePO_4/C$, and $LiFe_{0.96}V_{0.04}PO_4/C$ samples from 0.2 C to 10 C are shown in Fig.4. It is shown that the $LiFe_{0.96}V_{0.04}PO_4/C$ sample had a higher discharge capacity in comparison with the $LiFePO_4/C$ sample at a modest scope. The $LiFe_{0.96}V_{0.04}(PO_4)_{2.98/3}F_{0.02}/C$ sample revealed the best rate capability among three samples, especially under high rate conditions. It delivered a discharge capacity of 162.6 (0.2 C), 143.6 (0.5 C), 138.2 (1 C), 124.3 (2 C), 94 (5 C), 76.8

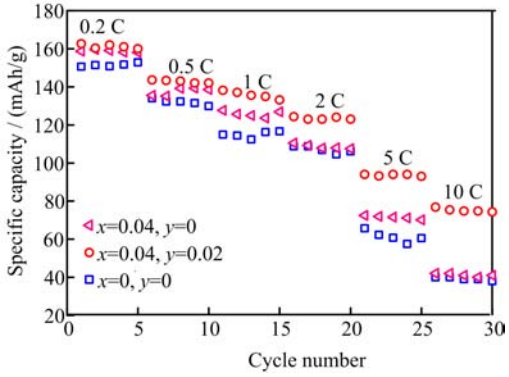

FIG. 4 The rate profiles of $LiFe_{1-x}V_x(PO_4)_{(3-y)/3}F_y/C$ composites.

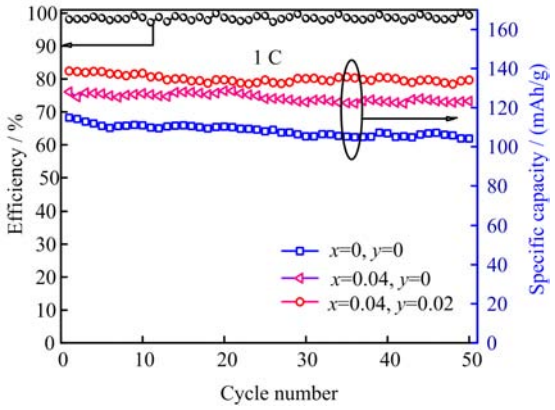

FIG. 5 Cycle performance profiles and coulombic efficiency of $LiFe_{1-x}V_x(PO_4)_{(3-y)/3}F_y/C$ at 1 C.

(10 C) mAh/g respectively. The capacity of the un-doped sample decreased dramatically with the rate increasing, remained only 40 mAh/g at 10 C, while the co-doped sample showed a capacity of 76.8 mAh/g at 10 C. The superior rate performance of $LiFe_{0.96}V_{0.04}(PO_4)_{2.98/3}F_{0.02}/C$ should result from the combined effects of V and F doping on the increasing conductivity of $LiFePO_4/C$.

Figure 5 shows cycle performances and coulombic efficiency of $LiFe_{1-x}V_x(PO_4)_{(3-y)/3}F_y/C$ at a current rate of 1 C. It can be observed that $LiFe_{0.96}V_{0.04}(PO_4)_{2.98/3}F_{0.02}/C$ displayed a higher capacity retention than that of $LiFePO_4/C$ and $LiFe_{0.96}V_{0.04}PO_4/C$ after 50 cycles. This indicated that the structural stability of $LiFePO_4/C$ was improved by V and F co-doping. The result was consistent with the conclusion about structure investigation. In addition, near 100% coulombic efficiency for $LiFe_{0.96}V_{0.04}(PO_4)_{2.98/3}F_{0.02}/C$ samples was achieved, which may be attributed to the fact that multicomponent doping leads to faster ion diffusion rate, and then slower capacity decay.

The Nyquist plots for $LiFePO_4/C$ and $LiFe_{0.96}V_{0.04}(PO_4)_{2.98/3}F_{0.02}/C$ samples are pre-

DOI:10.1063/1674-0068/29/cjcp1507163

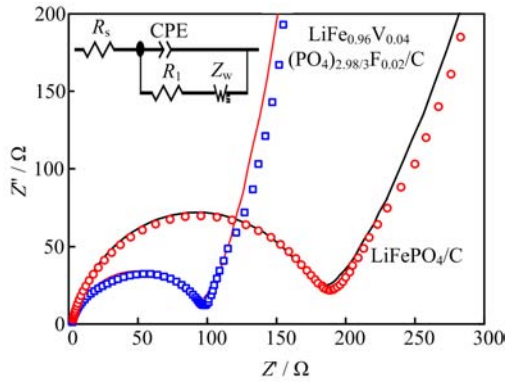

FIG. 6 EIS spectra of $LiFe_{0.96}V_{0.04}(PO_4)_{2.98/3}F_{0.02}/C$ and and $LiFePO_4/C$ electrodes. Solid lines show the fitting results.

sented in Fig.6. The high-frequency semicircle reacted to the charge transfer resistance (R_1), which was caused by charge transfer across the electrode electrolyte interface, whose diameter was approximately equal to the charge transfer resistance (R_1). The straight line at lower frequency presented Li^+ diffusion resistance in electrode bulk, namely, the Warburg impedance (Z_w), which was associated with Li ions diffusion in $LiFePO_4/C$ particles. As expected, the R_1 of $LiFePO_4/C$ electrode decreased in the charge/discharge process after V and F co-doping. The results indicate that the impedance of electrochemical reaction is improved by co-doping.

Figure 7 shows the CV curves of the second cycle at different scan rates between 0.1 and 0.6 mV/s within the potential window between 2.5−4.2 V. A couple of redox peaks corresponding to the lithium insertion and formation of $LiFePO_4/C$ phase were observed. Obviously, the peak shape of $LiFe_{0.96}V_{0.04}(PO_4)_{2.98/3}F_{0.02}/C$ was sharper and the peak separation was narrower than that of $LiFePO_4/C$.

At the same time, the diffusion coefficients of lithium ions (D_{Li^+}) in both samples were also calculated by CV, which was widely used to study the oxidation-reduction and phase transformation processes in electrode reactions and to estimate quantitatively D_{Li^+}. The corresponding fitting results are shown in Fig.8, it can be found that the redox peak currents of both $LiFePO_4/C$ and $LiFe_{0.96}V_{0.04}(PO_4)_{2.98/3}F_{0.02}/C$ electrodes showed a linear relationship with the square root of scan rate. For semi-infinite and finite diffusion, the peak current (i_p) was proportional to the square root of the scan rate and could be expressed by the classical Randles-Sevcik equation [45]:

$$i_p = 2.69 \times 10^5 n^{3/2} A C_0 D^{1/2} v^{1/2} \quad (1)$$

where n is the number of electrons involved in the redox process, A is the electrode area, C_0 was the molar concentration of lithium ions, D is the diffusion coefficient of lithium ions, and v is the potential scan rate.

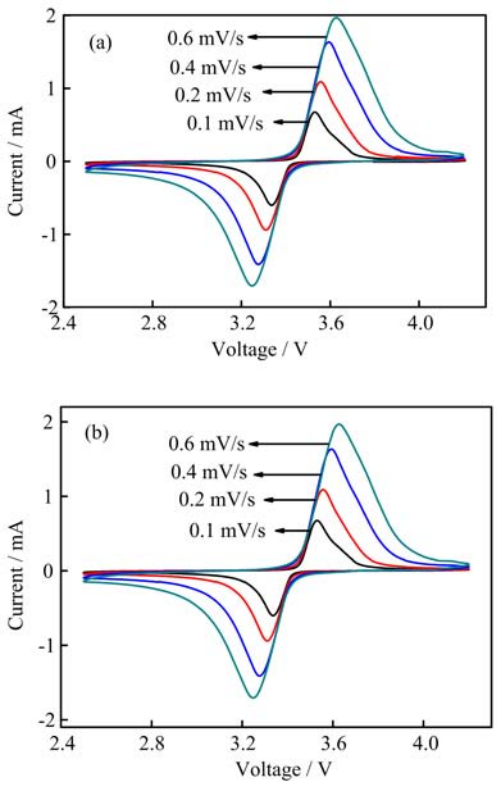

FIG. 7 CV curves of $LiFePO_4/C$ (a) and $LiFe_{0.96}V_{0.04}(PO_4)_{2.98/3}F_{0.02}/C$ (b) at different scan rate.

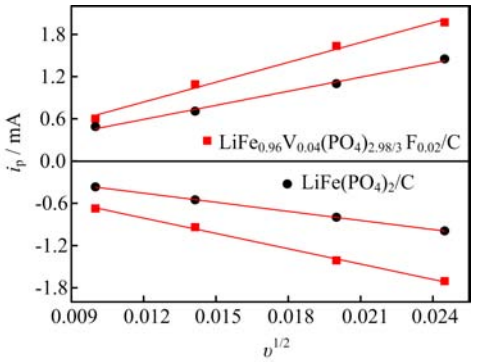

FIG. 8 Relationship of the peak current (i_p) and the square root of scan rate ($v^{1/2}$).

Based on the equation and the slope of i_p *vs.* $v^{1/2}$ in Fig.8, we achieved the D_{Li^+} of co-doping and initial samples during oxidation process were 1.00×10^{-10} and 4.98×10^{-11} cm^2/s. Obviously, V and F co-doping increased Li^+ diffusion coefficient of $LiFePO_4/C$.

IV. CONCLUSION

In this work, vanadium and fluorine co-doped $LiFePO_4/C$ cathode materials with uniform size and spherical morphology were synthesized via *in situ* poly-

DOI:10.1063/1674-0068/29/cjcp1507163

merization method combined with two-step sintering route. The V and F ions were successfully doped into the $LiFePO_4/C$ phase. The co-doping of V and F ions can enhance the structural stability, decrease charge transfer resistance, increase electronic conductivity, improve Li ion diffusion velocity, and finally result in eminent cycling and high-rate capabilities of $LiFePO_4/C$. Therefore, it can be concluded that the vanadium and fluorine co-doping was an effective way to improve the electrochemical performances of $LiFePO_4/C$ cathode materials for lithium-ion batteries.

V. ACKNOWLEDGMENTS

This work was supported by the National Natural Science Foundation of China (No.51364008), the Science and Technology Research Projects of Guangxi institution of higher education (No.2013ZD030), and the Guangxi Natural Science Foundation (No.2014GXNSFAA118046).

[1] M. Armand and J. M. Tarascon, Nature **451**, 652 (2008).
[2] P. Gibot, M. Casas-Cabanas, L. Laffont, S. Levasseur, P. Carlach, and J. M. Tarascon, Nature Mater. **7**, 741 (2008).
[3] A. Padhi, K. S. Nanjundaswamy, C. Masquelier, S. Okada, and J. B. Goodenough, J. Electrochem. Soc. **144**, A1609 (1997).
[4] M. Zhong and Z. Zhou, Solid State Ionics **181**, 1607 (2010).
[5] T. Nagakane, H. Yamauchi, K. Yuki, M. Ohji, A. Sakamoto, T. Komatsu, H. Honma, M. Zou, G. Park, and T. Sakai, Solid State Ionics **206**, 78 (2012).
[6] J. H Yum, E. Baranoff, S. Wenger, and M. K. Nazeeruddin, Energy Environ. Sci. **4**, 842 (2011).
[7] Y. G. Wang, P. He, and H. Zhou, Energy Environ. Sci. **4**, 805 (2011).
[8] J. Y. Li, W. L. Yao, S. Martin, and D. Vakin, Solid State Ionics **179**, 2016 (2008).
[9] G. Atnold, J. Garche, R. Hemmer, S. Strobele, C. Vogler, and M. Wohlfahrt Mehrens, J. Power Sources **119**, 247 (2003).
[10] V. Srinivasan and J. Newman, J. Electrochem. Soc. **151**, A1517 (2004).
[11] K. Rissouli, K. Benkhouja, J. R. Ramos-Barrado, and C. Julien, Mater. Sci. Eng. B **98**, 185 (2003).
[12] M. Gaberscek, R. Dominko, and J. Jamnik, Electrochem. Commun. **9**, 2778 (2007).
[13] P. P. Prosini, M. Lisi, and D. Zane, Solid State Ionics **45**, 148 (2002).
[14] R. Dominko, M. Gaberscek, J. Drofenik, M. Bele, S. Pejovnik, and J. Jamnik, J. Power Sources **119**, 770 (2003).
[15] N. Ravet, Y. Chouinard, J. F. Magnan, S. Besner, M. Gauthier, and M. Armand, J. Power Sources **97**, 503 (2001).
[16] F. F. Pan, W. L. Wang, D. M. Chen, and W. S. Yan, J. Mater. Chem. **21**, 14680 (2011).
[17] F. F. Pan, W. L. Wang, H. J. Li, and X. D. Xin, Electrochim. Acta **56**, 6940 (2011).
[18] Q. Q. Chang, G. H. Yao, F. F. Pan, and D. M. Chen, Electrochim. Acta **108**, 211 (2013).
[19] W. J. Zhang, J. Power Sources **196**, 2962 (2011).
[20] R. Malik, D. Burch, M. Bazant, and G. Ceder, Nano Lett. **10**, A4123 (2010).
[21] X. Q. Ou, H. C. Gu, Y. C. Wu, J. W. Lu, and Y. J. Zheng, Electrochim. Acta **96**, 230 (2013).
[22] J. Hong, X. L. Wang, Q. Wang, and F. Omenya, J. Phys. Chem. C **116**, 20787 (2012).
[23] H. Y. Gao, L. F. Jiao, W. X. Peng, and G. Liu, Electrochim. Acta **56**, 9961 (2011).
[24] Z. H. Wang, L. X. Yuan, J. Ma, L. Qie, and L. Zhang, Electrochim. Acta **62**, 416 (2012).
[25] L. Wang, H. Wang, Z. Liu, C. Xiao, and S. Dong, Solid State Ionics **181**, 1685 (2010).
[26] J. Wang, Z. Shao, and H. Ru, Ceram. Int. **40**, 6979 (2014).
[27] K. Park, S. Schougaard, and J. Goodenough, Adv. Mater. **19**, 848 (2007).
[28] G. Qin, Q. Ma, and C. Wang, Solid State Ionics **257**, 60 (2014).
[29] M. Abbate, S. M. Lala, L. A. Montoro, and J. M. Rosolenb, Electrochem. Solid State Lett. **8**, A288 (2005).
[30] Z. H. Wang, Q. Q. Pang, J. K. Deng, and L. X. Yuan, Electrochim. Acta **78**, 576 (2012).
[31] Z. Liu, X. Huang, and D. Wang, Solid State Commun. **147**, 505 (2008).
[32] L. Yang, L. Jiao, Y. Miao, and H. Yuan, J. Solid State Electrochem. **13**, 1541 (2009).
[33] X. Liao, Y. He, and Z. Ma, J. Power Sources **174**, 720 (2007).
[34] R. Malik, D. Burch, M. Bazant, and G. Ceder, Nano Lett. **10**, 4123 (2010).
[35] F. Lu, Y. C. Zhou, J. Liu, and Y. Pan, Electrochim. Acta **56**, 8833 (2011).
[36] F. Pan and W. L. Wang, J. Solid State Electrochem. **16**, 1423 (2012).
[37] M. Milović, D. Jugović, N. Cvjetićanin, and D. Uskoković, J. Power Sources **241**, 70 (2013).
[38] D. Wang, H. Li, and Z. Wang, J. Solid State Chem. **177**, 4582 (2004).
[39] B. Wu, Y. Zhang, and N. Li, J. New Mater. Electrochem. Syst. **14**, 147 (2011).
[40] G. Amatucci and N. Pereira, J. Fluor. Chem. **128**, 243 (2007).
[41] X. Z. Liao, Y. S. He, Z. F. Ma, and X. M. Zhang, J. Power Sources **174**, 720 (2011).
[42] M. Yang and W. Ke, J. Electrochem. Soc. **155**, A729 (2008).
[43] T. Teng, M. Yang, and S. Wu, Solid State Commun. **142**, 389 (2007).
[44] A. Salah, P. Jozwiak, and J. Garbarczyk, J. Power Sources **140**, 370 (2005).
[45] J. Dahn, J. Jiang, and L. Moshurchak, J. Electrochem. Soc. **152**, A1283 (2005).

DOI:10.1063/1674-0068/29/cjcp1507163